

Search for the evaporation of primordial black holes with H.E.S.S.

F. Aharonian,^{1,2} F. Ait Benkhali,³ J. Aschersleben,⁴ M. Böttcher,⁵
M. Backes,^{6,5} V. Barbosa Martins,⁷ R. Batzofin,⁸ Y. Becherini,^{9,10}
D. Berge,^{7,11} B. Bi,¹² C. Boisson,¹³ J. Bolmont,¹⁴
M. de Bony de Lavergne,¹⁵ J. Borowska,¹¹ F. Bradascio,¹⁶
R. Brose,¹ F. Brun,¹⁶ B. Bruno,¹⁷ T. Bulik,¹⁸ C. Burger-Scheidlin,¹
S. Caroff,¹⁴ S. Casanova,¹⁹ J. Celic,¹⁷ M. Cerruti,⁹ T. Chand,⁵
A. Chen,⁸ O. Chibueze,⁵ G. Cotter,²⁰
J. Damascene Mbarubucyeye,⁷ A. Djannati-Ataï,⁹ K. Egberts,²¹
C. van Eldik,¹⁷ J.-P. Ernenwein,²² M. Füßling,⁷ A. Fiasson,¹⁵
G. Fichet de Clairfontaine,¹³ G. Fontaine,²³ S. Gabici,⁹
S. Ghafourizadeh,³ G. Giavitto,⁷ D. Glawion,¹⁷ J.F. Glicenstein,¹⁶
G. Grolleron,¹⁴ M.-H. Grondin,²⁴ L. Haerer,² M. Haupt,⁷
J.A. Hinton,² W. Hofmann,² M. Holler,²⁵ D. Horns,²⁶
Zhiqiu Huang,² M. Jamrozy,²⁷ F. Jankowsky,³ V. Joshi,¹⁷
I. Jung-Richardt,¹⁷ E. Kasai,⁶ K. Katarzyński,²⁸ B. Khélifi,⁹
S. Klepser,⁷ W. Kluźniak,²⁹ Nu. Komin,⁸ K. Kosack,¹⁶
D. Kostunin,⁷ T. L. Holch,⁷ R.G. Lang,¹⁷ S. Le Stum,²² F. Leitzl,¹⁷
A. Lemièrre,⁹ J.-P. Lenain,¹⁴ F. Leuschner,¹² T. Lohse,¹¹
A. Luashvili,¹³ I. Lypova,³ J. Mackey,¹ D. Malyshev,¹⁷
V. Marandon,² P. Marchegiani,⁸ P. Marinos,³⁰ G. Martí-Devesa,²⁵
R. Marx,³ A. Mitchell,^{17,2} R. Moderski,²⁹ L. Mohrmann,²
A. Montanari,¹⁶ E. Moulin,¹⁶ J. Muller,²³ K. Nakashima,¹⁷
M. de Naurois,²³ J. Niemiec,¹⁹ P. O'Brien,³¹ S. Ohm,⁷
L. Olivera-Nieto,² E. de Ona Wilhelmi,⁷ M. Ostrowski,²⁷
G. Pühlhofer,¹² S. Panny,²⁵ M. Panter,² R.D. Parsons,¹¹ G. Peron,²
A. Priyana Noel,²⁷ D.A. Prokhorov,³² H. Prokoph,⁷ M. Punch,^{9,10}
A. Quirrenbach,³ P. Reichherzer,¹⁶ O. Reimer,²⁵ F. Rieger,²
G. Rowell,³⁰ B. Rudak,²⁹ H. Rueda Ricarte,¹⁶ V. Sahakian,³³
H. Salzmann,¹² D.A. Sanchez,¹⁵ A. Santangelo,¹² M. Sasaki,¹⁷
H.M. Schutte,⁵ U. Schwanke,¹¹ J.N.S. Shapopi,⁶ H. Sol,¹³
A. Specovius,¹⁷ S. Spencer,¹⁷ Ł. Stawarz,²⁷ R. Steenkamp,⁶

**S. Steinmassl,² C. Steppa,²¹ I. Sushch,⁵ H. Suzuki,³⁴
T. Takahashi,³⁵ T. Tanaka,³⁴ T. Tavernier,¹⁶ C. Thorpe-Morgan,¹²
N. Tsuji,³⁶ Y. Uchiyama,³⁷ M. Vecchi,⁴ J. Veh,¹⁷ C. Venter,⁵
J. Vink,³² S.J. Wagner,³ R. White,² A. Wiercholska,¹⁹
Yu Wun Wong,¹⁷ M. Zacharias,^{13,5} D. Zargaryan,¹ A.A. Zdziarski,²⁹
A. Zech,¹³ S. Zouari,⁹ and N. Żywucka.⁵**

¹Dublin Institute for Advanced Studies, 31 Fitzwilliam Place, Dublin 2, Ireland

²Max-Planck-Institut für Kernphysik, P.O. Box 103980, D 69029 Heidelberg, Germany

³Landessternwarte, Universität Heidelberg, Königstuhl, D 69117 Heidelberg, Germany

⁴Kapteyn Astronomical Institute, University of Groningen, Landleven 12, 9747 AD Groningen, The Netherlands

⁵Centre for Space Research, North-West University, Potchefstroom 2520, South Africa

⁶University of Namibia, Department of Physics, Private Bag 13301, Windhoek 10005, Namibia

⁷DESY, D-15738 Zeuthen, Germany

⁸School of Physics, University of the Witwatersrand, 1 Jan Smuts Avenue, Braamfontein, Johannesburg, 2050 South Africa

⁹Université de Paris, CNRS, Astroparticule et Cosmologie, F-75013 Paris, France

¹⁰Department of Physics and Electrical Engineering, Linnaeus University, 351 95 Växjö, Sweden

¹¹Institut für Physik, Humboldt-Universität zu Berlin, Newtonstr. 15, D 12489 Berlin, Germany

¹²Institut für Astronomie und Astrophysik, Universität Tübingen, Sand 1, D 72076 Tübingen, Germany

¹³Laboratoire Univers et Théories, Observatoire de Paris, Université PSL, CNRS, Université de Paris, 92190 Meudon, France

¹⁴Sorbonne Université, Université Paris Diderot, Sorbonne Paris Cité, CNRS/IN2P3, Laboratoire de Physique Nucléaire et de Hautes Energies, LPNHE, 4 Place Jussieu, F-75252 Paris, France

¹⁵Université Savoie Mont Blanc, CNRS, Laboratoire d'Annecy de Physique des Particules - IN2P3, 74000 Annecy, France

¹⁶IRFU, CEA, Université Paris-Saclay, F-91191 Gif-sur-Yvette, France

¹⁷Friedrich-Alexander-Universität Erlangen-Nürnberg, Erlangen Centre for Astroparticle Physics, Erwin-Rommel-Str. 1, D 91058 Erlangen, Germany

¹⁸Astronomical Observatory, The University of Warsaw, Al. Ujazdowskie 4, 00-478 Warsaw, Poland

¹⁹Instytut Fizyki Jądrowej PAN, ul. Radzikowskiego 152, 31-342 Kraków, Poland

²⁰University of Oxford, Department of Physics, Denys Wilkinson Building, Keble Road, Oxford OX1 3RH, UK

²¹Institut für Physik und Astronomie, Universität Potsdam, Karl-Liebknecht-Strasse 24/25, D 14476 Potsdam, Germany

²²Aix Marseille Université, CNRS/IN2P3, CPPM, Marseille, France

²³Laboratoire Leprince-Ringuet, École Polytechnique, CNRS, Institut Polytechnique de Paris, F-91128 Palaiseau, France

- ²⁴Université Bordeaux, CNRS, LP2I Bordeaux, UMR 5797, F-33170 Gradignan, France
- ²⁵Institut für Astro- und Teilchenphysik, Leopold-Franzens-Universität Innsbruck, A-6020 Innsbruck, Austria
- ²⁶Universität Hamburg, Institut für Experimentalphysik, Luruper Chaussee 149, D 22761 Hamburg, Germany
- ²⁷Obserwatorium Astronomiczne, Uniwersytet Jagielloński, ul. Orła 171, 30-244 Kraków, Poland
- ²⁸Institute of Astronomy, Faculty of Physics, Astronomy and Informatics, Nicolaus Copernicus University, Grudziadzka 5, 87-100 Torun, Poland
- ²⁹Nicolaus Copernicus Astronomical Center, Polish Academy of Sciences, ul. Bartycka 18, 00-716 Warsaw, Poland
- ³⁰School of Physical Sciences, University of Adelaide, Adelaide 5005, Australia
- ³¹Department of Physics and Astronomy, The University of Leicester, University Road, Leicester, LE1 7RH, United Kingdom
- ³²GRAPPA, Anton Pannekoek Institute for Astronomy, University of Amsterdam, Science Park 904, 1098 XH Amsterdam, The Netherlands
- ³³Yerevan Physics Institute, 2 Alikhanian Brothers St., 375036 Yerevan, Armenia
- ³⁴Department of Physics, Konan University, 8-9-1 Okamoto, Higashinada, Kobe, Hyogo 658-8501, Japan
- ³⁵Kavli Institute for the Physics and Mathematics of the Universe (WPI), The University of Tokyo Institutes for Advanced Study (UTIAS), The University of Tokyo, 5-1-5 Kashiwanoha, Kashiwa, Chiba, 277-8583, Japan
- ³⁶RIKEN, 2-1 Hirosawa, Wako, Saitama 351-0198, Japan
- ³⁷Department of Physics, Rikkyo University, 3-34-1 Nishi-Ikebukuro, Toshima-ku, Tokyo 171-8501, Japan

Abstract.

Primordial Black Holes (PBHs) are hypothetical black holes predicted to have been formed from density fluctuations in the early Universe. PBHs with an initial mass around $10^{14} - 10^{15}$ g are expected to end their evaporation at present times in a burst of particles and very-high-energy (VHE) gamma rays. Those gamma rays may be detectable by the High Energy Stereoscopic System (H.E.S.S.), an array of imaging atmospheric Cherenkov telescopes. This paper reports on the search for evaporation bursts of VHE gamma rays with H.E.S.S., ranging from 10 to 120 seconds, as expected from the final stage of PBH evaporation and using a total of 4816 hours of observations. The most constraining upper limit on the burst rate of local PBHs is $2000 \text{ pc}^{-3} \text{ yr}^{-1}$ for a burst interval of 120 seconds, at the 95% confidence level. The implication of these measurements for PBH dark matter are also discussed.

Contents

1	Introduction	1
2	H.E.S.S. array and data set	2
3	Expected PBH signal	2
4	Data analysis	4
4.1	Clustering algorithm	5
4.2	Background estimation	5
4.3	Statistical methods	6
5	Results and discussion	7
5.1	Cluster distributions	7
5.2	Discussion	7
6	Conclusions	10

1 Introduction

Primordial black holes (PBHs) [1] have been predicted to form in the early Universe via a variety of mechanisms [2]. The gravitational collapse of over-dense regions with significant density fluctuations [3] is the best known of these mechanisms. It requires a spectrum of primordial density fluctuations with an excess of power on small spatial scales to be efficient. Other formation mechanisms include pressure reduction during cosmological phase transitions [4]. The mass function of PBHs depends on the actual formation mechanism. PBHs could have masses ranging from 10^{-5} g for PBHs created at the Planck time up to several tens of M_{\odot} for PBHs created during the QCD phase transition [4]. No PBH candidate has been unambiguously detected, although recent black hole merging events [5] and Massive Compact Halo Objects (MACHOs) [4] could be explained with PBHs.

Black holes were predicted by Hawking [6] to radiate particles with a black body spectrum of effective temperature

$$T_{\text{BH}} = \frac{M_p^2}{8\pi M_{\text{BH}}}, \quad (1.1)$$

where M_p and M_{BH} are the Planck mass and the PBH mass, respectively. In equation (1.1) and in the following, the temperature and the masses are written in energy units, the constants k_B , \hbar and c are all set to 1. Hawking's radiation is negligible for black holes of stellar masses or higher. However evaporation becomes the predominant process that governs the black hole evolution for small-mass black holes. Black holes lose their mass by Hawking radiation at a rate inversely proportional to their squared mass.

A popular method for constraining the density of low-mass PBHs is searching for their gamma-ray emission. Searches have attempted to detect a diffuse photon signal from a distribution of PBHs [7] or to look directly for the final stage emission of an individual hole [8–10].

The present paper reports on the search for TeV gamma-ray bursts with a timescale of a few seconds to a few minutes [11], as expected from the final stage of PBHs evaporation, using the H.E.S.S. array of Imaging Atmospheric Cherenkov Telescopes (IACTs). The H.E.S.S. data selection and processing are presented in Sec. 2. The modelling of the PBH signal is described in Sec. 3. The burst search algorithm and background estimation are discussed in Sec. 4. The results on the local evaporation rate, and the comparison to existing limits are given in Sec. 5.1. The implication of the obtained results on PBH dark matter is discussed in Sec. 5.2. Finally, conclusions are drawn in Sec. 6.

2 H.E.S.S. array and data set

The High Energy Stereoscopic System (H.E.S.S.) is an array of five imaging atmospheric Cherenkov telescopes dedicated to observing very-high-energy (VHE; $\gtrsim 100$ GeV) gamma rays from astrophysical sources. It is located in the Khomas Highland of Namibia at an altitude of 1800 m above sea level. The first four telescopes were installed in 2001-2003 (H.E.S.S.1 phase of the experiment) and have been operational since 2004. Each telescope of H.E.S.S.1 is equipped with a tessellated optical reflector of 107 m^2 [12] and a camera with 960 photomultiplier tubes. The camera field of view is 5° in diameter. The stereoscopic technique [13] allows for an accurate reconstruction of the direction and the energy of the primary gamma ray. H.E.S.S.1 has an angular resolution of less than 0.1° , a source location accuracy of $\sim 30''$ for strong sources and an effective detection area of $\sim 10^5 \text{ m}^2$. The sensitivity for point-like sources reaches $2 \times 10^{-13} \text{ cm}^{-2}\text{s}^{-1}$ above 1 TeV for a 5σ detection in 25 hours of a source at a 20° zenith angle [14]. The fifth telescope with a reflective area of 614 m^2 , which started its operations in 2012, is not used in this analysis.

The data used for this analysis are the vast majority of the H.E.S.S. observations taken between January 2004 and January 2013. Each observation is called a run and consists of data taken pointing towards the same position in the sky during ~ 28 minutes. The runs with poor quality (due to hardware problems, bad atmosphere, etc...) as well as those with large zenith angle ($> 60^\circ$) were removed in order to reduce the systematic uncertainties. This yields a total of 11234 runs which corresponds to 4816 hours. The event reconstruction (direction, energy) has been performed using the ImPACT method [15] and the identification of background events was done using boosted decision trees [16]. Events with a distance to the center of the camera larger than 2° are excluded. In addition, events for which the energy bias is estimated to be above 10% are excluded, defining a safe energy range for each run. The results were cross-checked with a different calibration and event reconstruction pipelines [14], giving consistent results.

3 Expected PBH signal

To discover or constrain PBH evaporation, observations have to be compared to models. During the evaporation process, the PBH heats up by emitting particles with masses around and below its temperature. The prediction of the instantaneous gamma-ray spectrum $d^2N/dE_\gamma dt$ emitted by the PBH in its last seconds depends on the assumed elementary particle mass spectrum and more generally on the extrapolation of known physics to large PBH temperatures [11]. In the hadronic model of Hagedorn [17], temperature is limited by an ultimate value of $\simeq 160$ MeV. In this model, the signature of PBH evaporation is a microsecond burst of photons with energies $\simeq 100$ MeV [18]. In loop quantum gravity, the PBH might

explode before total evaporation, leading to short ~ 10 MeV bursts [19]. In the more standard MacGibbon-Webber model [20], the black hole emits only those Standard Model species which appear fundamental on the scale of the black hole temperature, decaying and hadronizing as they stream away from the black hole, and so PBH temperatures in the TeV range can be reached. In supersymmetric particle models, additional degrees of freedom tend to accelerate the PBH evaporation [21]. The gamma rays detectable by H.E.S.S. are emitted when the PBH has a temperature in the 100 GeV-10 TeV energy range. It is assumed in this paper that the standard model of particle physics remains valid in the H.E.S.S. temperature range. Another systematic effect in the modelling is the presence of a photosphere around the PBH [22, 23], which would drastically alter the evaporation signal by suppressing the high-energy component of emitted particles. However, photospheric effects around PBHs are under debate [24]. In this paper, possible PBH photosphere effects on the evaporation signal have been neglected.

Following the analysis in [11] and [25], the integrated spectrum of photons per square meter emitted during the time Δt before total evaporation of the PBH and observed by a detector at a distance r_0 is given by :

$$N(> E) = 0.22 \left(\frac{0.1 \text{ pc}}{r_0} \right)^2 \left(\frac{\text{TeV}}{Q} \right)^2 \left(\frac{5}{14} \left(\frac{E}{Q} \right)^{\frac{3}{2}} + 3 \left(\frac{E}{Q} \right)^{1/2} + \frac{5}{6} \left(\frac{Q}{E} \right)^{1/2} - \frac{5}{3} \left(\frac{E}{Q} \right) - \frac{5}{2} + \frac{1}{150} \right), \quad (3.1)$$

for $E < Q$ and by :

$$N(> E) = 0.22 \left(\frac{0.1 \text{ pc}}{r_0} \right)^2 \left(\frac{\text{TeV}}{E} \right)^2 \left(\frac{1}{42} + \frac{1}{150} \right), \quad (3.2)$$

for $E \geq Q$. In the above equations, E is the energy, and Q relates to Δt by:

$$Q \simeq 40 \text{ TeV} (1 \text{ s}/\Delta t)^{1/3}. \quad (3.3)$$

Q is a slowly decreasing function of Δt , with values for the observations reported in this paper ranging from ~ 8 TeV for $\Delta t = 120$ seconds to ~ 13 TeV for $\Delta t = 30$ seconds. H.E.S.S. is sensitive to PBH evaporations up to distances of order $r_0 = 0.1$ pc, so that the expected flux does not need to be corrected for Extragalactic Background Light (EBL) absorption.

Instead of equation 3.1, the low-energy asymptotic form

$$N(> E) = 0.18 \left(\frac{0.1 \text{ pc}}{r_0} \right)^2 \left(\frac{\text{TeV}}{Q} \right)^2 \left(\frac{Q}{E} \right)^{1/2} \quad (3.4)$$

was used in the predictions for convenience. This simple power-law form is very close to the fit of the MacGibbon-Weber model [20] given in [26]. Equations 3.1-3.4 can be simply understood as describing a broken power-law spectrum with a low-energy photon index of $\frac{5}{2}$, a high-energy photon index of 3 and a break energy of Q .

Our spectrum, when compared to more recent analytical calculations in [21] and to the output of the public BlackHawk program [27], shows a consistency at the factor of 2 level in the H.E.S.S. energy range.

The theoretical average number of gamma rays detected from a PBH located at a distance r_0 and direction (α_0, δ_0) in the sky, during the last Δt seconds of its life is given by:

$$N_\gamma(r_0, \alpha_0, \delta_0, \Delta t) = \int_0^\infty dE_\gamma \frac{dN(\Delta t)}{dE_\gamma} A(E_\gamma, \alpha_0, \delta_0), \quad (3.5)$$

where $N(\Delta t) = N(> E)$ is defined in equations 3.2 and 3.4. The break energy Q increases during PBH's life and is larger than 1 TeV in the last ~ 18 hours. However, equations 3.3 and 3.4 show that the number of gamma rays from PBH evaporation scales like $\sqrt{\Delta t}$ while the background increases linearly with Δt . Because of this, in practice, the optimal time-window Δt for the search with H.E.S.S. is in the range of a few to a few tens of seconds. The signature of a PBH evaporation is thus a burst of high-energy photons lasting a few seconds.

The evaporation photon spectrum has to be folded with the H.E.S.S. effective area $A(E_\gamma, \alpha_0, \delta_0)$ to take into account the instrument's efficiency in collecting gamma rays of energy E_γ at equatorial coordinates (α_0, δ_0) in the sky. The response of the H.E.S.S. instrument to gamma rays depends on the zenith angle and the event's offset to the camera center.

The probability of detecting a burst of size¹ b when observing a PBH with expected number of detected gamma rays $N_\gamma(r_0, \alpha_0, \delta_0, \Delta t)$ follows the Poisson statistics:

$$P(b, N_\gamma) = e^{-N_\gamma} \frac{N_\gamma^b}{b!}. \quad (3.6)$$

Integrating this probability over all space and assuming an isotropic distribution of PBH sources gives the theoretical number of expected bursts of size b to be detected in the data for an observation run i :

$$n_{sig}^i(b, \Delta t, \dot{\rho}_{PBH}) = \dot{\rho}_{PBH} V_{eff}^i(b, \Delta t), \quad (3.7)$$

where $\dot{\rho}_{PBH}$ is the local PBH evaporation burst rate per unit volume and the effective space-time volume of PBH detection is defined by

$$V_{eff}^i(b, \Delta t) = t_i \int d\Omega_i \int_0^\infty dr r^2 P_i(b, N_\gamma), \quad (3.8)$$

where the index i goes over each run of the H.E.S.S. data set, t_i and $d\Omega_i$ being the corresponding run live time and observation solid angle, respectively.

The effective volume can be written explicitly as

$$V_{eff}^i(b, \Delta t) = t_i \Omega_i \frac{(r_0 \sqrt{N_0})^3}{2} \frac{\Gamma(b - 3/2)}{\Gamma(b + 1)}, \quad (3.9)$$

where N_0 is the expected number of photons from a PBH at r_0 and Γ is Euler's gamma function.

4 Data analysis

The signature of a PBH evaporation is thus a burst of a small number (≥ 2) of gamma-like events which arrive in coincidence in angular space and time within a few seconds. This section describes the algorithm used to find the photon clusters in the H.E.S.S. data set, the estimation of the background rate and the statistical methods used to put constraints on the PBH evaporation rate.

¹In the following, the number of gamma rays detected in a burst is named the size of the burst

4.1 Clustering algorithm

The clustering method used in this paper is based on the OPTICS (Ordering Points To Identify the Clustering Structure) algorithm [28] implemented in the scikit-learn library [29]. OPTICS is an improved version of DBSCAN [30] which builds clusters step by step, grouping points that are closely packed together given a predefined maximum distance. Three parameters are required for DBSCAN: ϵ_θ , the maximum angular distance on the sky between two points, ϵ_t , the maximum duration between two events and MinPts, the minimum number of events to declare a cluster. In this analysis, MinPts has been set to 2, ϵ_t to Δt and ϵ_θ to 0.14° , which is twice the integration radius used in the point-like analysis with ImPACT reconstruction. OPTICS is more flexible than DBSCAN and allows finding clusters in a variable density environment. It finds core samples of high density and expands clusters from them. OPTICS uses a fourth parameter ξ which defines the density steepness at the cluster boundary. The parameter ξ has been set to the default value $\xi = 0.05$.

Clusters found may be spatially larger than the point-like integration radius or last longer than the chosen Δt . When this happens, photon events from the cluster which are distant from the cluster median position in angle by more than this radius are excluded. The procedure is iterated until the cluster smallest enclosing circle reaches this radius, which makes it then comparable to the effective area derived by Monte-Carlo simulations (cf equation 3.5). The same procedure is performed in the time dimension.

After excluding photons from large clusters, it happens that some groups of photon events still follow our cluster definition. A second pass of this same algorithm is then applied to the remaining events. The whole cluster-finding procedure was validated by injecting simulated clusters of photons in the data. The cluster-finding efficiency is estimated to be $\simeq 98\%$ for 5-photon clusters.

4.2 Background estimation

Random fluctuations are expected to induce photon clusters by chance. It is therefore crucial to calculate the random cluster background with the best possible accuracy. The strategy followed in this paper is the direct estimation of the background from the data, by using the same photon list, but with randomized (“scrambled”) times of arrival. The average value of the number of clusters distribution obtained by time scrambling 200 times the photon list of each run (except for some runs, for which the number was increased to 1000) is taken as the background. In the rest of the paper, the set of time-randomized photons will be referred to as OFF data. For a given cluster size, the number of clusters found in the OFF data follows a Poisson distribution, as illustrated in Fig. 1.

The chance association of gamma-like events to form a cluster is a decreasing function of the photon cluster size. Therefore the OFF data are not sufficient to accurately predict the statistical background of large photon clusters. To obtain the background value in that case, the distribution of the mean number of photon clusters is fitted with a power-law distribution with an exponential cut off :

$$N(b) = A b^s e^{-tb}. \quad (4.1)$$

The extrapolation of this equation is used to obtain the mean of the Poisson probability distribution of cluster sizes for large cluster sizes. Figure 2 shows an example of the distribution of cluster sizes for a H.E.S.S. run.

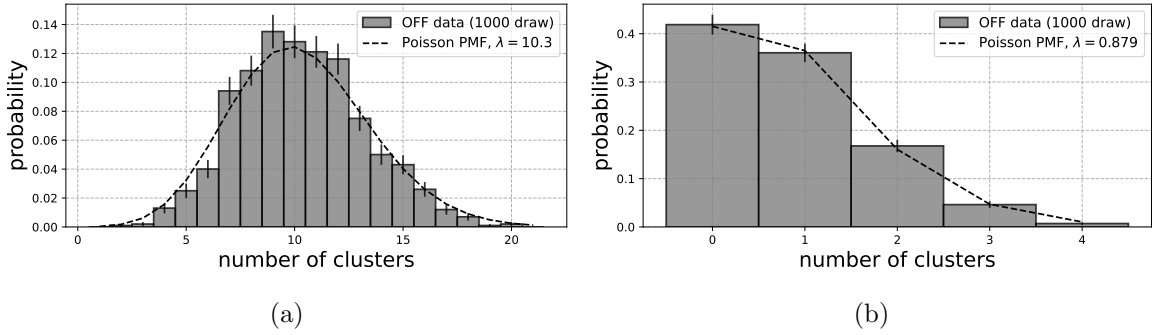


Figure 1: Calculation of the statistical background for 60-second clusters of $b = 4$ (a) and $b = 5$ (b) photons. The photon list of a 28-minute H.E.S.S. run was time-scrambled 1000 times instead of the more usual 200 times. A Poisson law (dashed line) with an expected mean value λ equal to the measured value in the OFF data is superimposed.

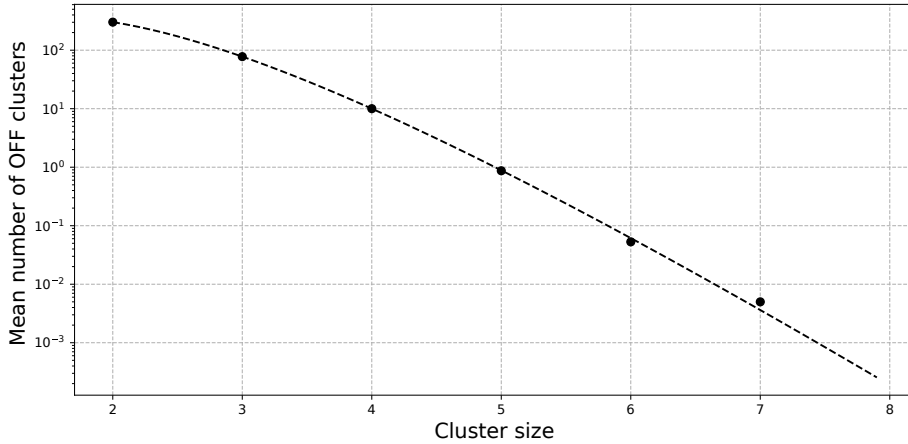


Figure 2: Distribution of the mean number of 60-second clusters found in 1000-time randomisation of a run (black dots). This distribution is fitted with a power-law with an exponential cut off (equation 4.1). The fitted distribution (black dashed line) is used to extrapolate the expected number of OFF clusters for large sizes.

4.3 Statistical methods

A hypothetical PBH signal is discovered or constrained by comparing the observed data to the expected background (hypothesis H_0). The predicted flux depends on the unknown number density of bursting PBH, ρ_{PBH} . If an evaporation signal exists in the data, both the evaporation signal and the background will be observed (hypothesis H_1). The PBH density is estimated by maximizing a likelihood ratio with $\dot{\rho}_{\text{PBH}}$ as the only free parameter, following the procedure of Feldman-Cousins [31]. The likelihood ratio is given by:

$$\frac{\mathcal{L}_{H_1}}{\mathcal{L}_{H_0}} = \prod_i \frac{\mathcal{P}(n_{\text{ON}}^i | \lambda = n_{\text{OFF}}^i + n_{\text{sig}}^i(b, \Delta t, \dot{\rho}_{\text{PBH}}))}{\mathcal{P}(n_{\text{ON}}^i | \lambda = n_{\text{OFF}}^i)}, \quad (4.2)$$

where \mathcal{P} is the Poisson probability, $n_{\text{sig}}^i(b, \Delta t, \dot{\rho}_{\text{PBH}})$ is defined in equation 3.7, n_{ON}^i is the number of clusters found in the data and n_{OFF}^i is the corresponding mean number of clusters

found in the OFF data.

The corresponding test statistic is given by:

$$TS = -2 \ln \left(\frac{\mathcal{L}_{H_0}}{\mathcal{L}_{H_1}} \right) = -2 \times \sum_i [n_{sig}^i + n_{ON}^i (\ln(n_{OFF}^i) - \ln(n_{OFF}^i + n_{sig}^i))] . \quad (4.3)$$

Another model-independent way to compare the data to the expected background is to look for a cluster excess of a given cluster size. For each time scale, Δt , and cluster size, b , the model-independent maximum-likelihood ratio test is given by

$$\frac{\mathcal{L}_{H_1}(b)}{\mathcal{L}_{H_0}(b)} = \prod_i \frac{\mathcal{P}(n_{ON}^i(b) | \lambda = n_{OFF}^i(b) + n)}{\mathcal{P}(n_{ON}^i(b) | \lambda = n_{OFF}^i(b))} , \quad (4.4)$$

where n is the excess of clusters. Maximisation on the free parameter n gives a model-independent estimation of the measured cluster excess for each cluster size, b .

5 Results and discussion

5.1 Cluster distributions

As discussed in section 3, the size of the timescale Δt is constrained by the statistical background. Therefore, the analysis was performed for 4 values of the timescale Δt , namely 10, 30, 60 and 120 seconds, using the 4816 hours data set described in section 2. The lack of cluster statistics makes the background estimation difficult for timescales lower than 10 seconds. The CPU load of the clustering algorithm increases with Δt which led to limit the analysis to $\Delta t \leq 120$ seconds. The difference between the number of clusters found in the ON and OFF data sets, as well as the fitted excess, obtained from the likelihood ratio 4.2, and the 99% upper limits on a cluster excess, derived from the likelihood ratio 4.4, are shown in Figure 3 for $\Delta t = 60$ s.

No significant signal was found in the data. Upper limits on the PBH evaporation burst rate $\dot{\rho}_{PBH}$ with confidence levels (CL) of 95% and 99% were derived by finding the $\dot{\rho}_{PBH}$ for which $TS = 3.84$ and 6.63 respectively. These upper limits are shown in Fig. 4 and compared to the limits obtained by HAWC [10], VERITAS [8], Milagro [32] and Fermi-LAT [9]. Note that the limits depend on the predicted photon flux. The predictions used by H.E.S.S. are in fair agreement with those used by the other Cherenkov arrays and with those of the BlackHawk program [27]. The Fermi-LAT result, which is derived from lower energy photons, uses a $\simeq 40\%$ smaller photon flux. The upper limits are inversely proportional to the effective volume (equation 3.9). A factor of 2 uncertainty in the predicted photon flux from a PBH evaporation translates into a factor 3 uncertainty in the limits.

5.2 Discussion

The time evolution of PBH masses is given by

$$\frac{dM}{dt} = -\frac{\alpha(M)}{M^2} , \quad (5.1)$$

where $\alpha(M)$ counts the degrees of freedom of the particles contributing to the energy loss as a function of the black-hole mass [11]. The low-mass limit of the function $\alpha(M)$ strongly

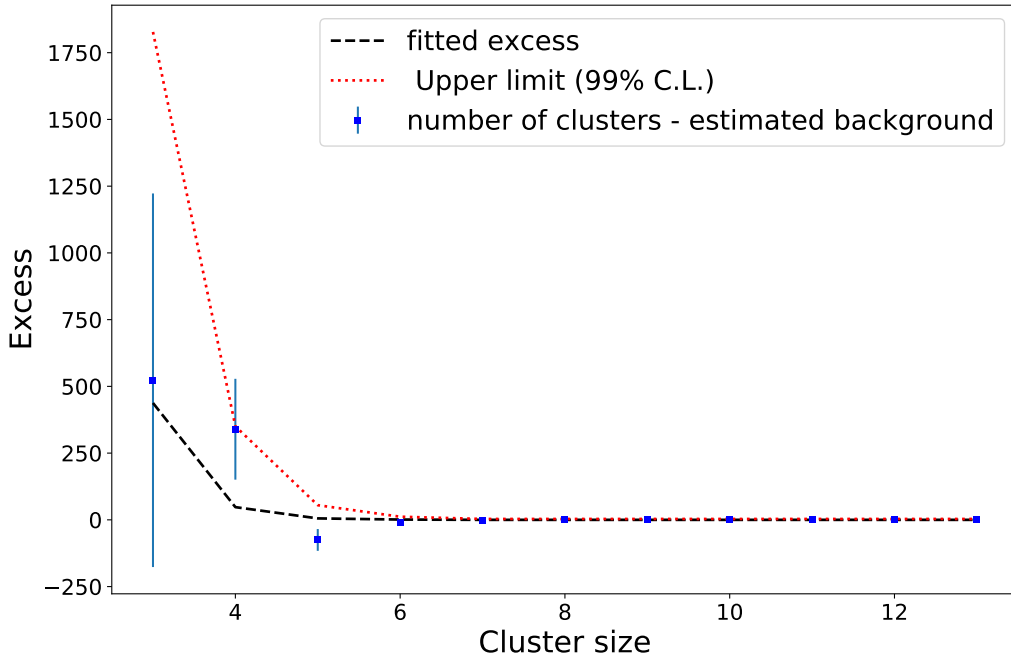


Figure 3: Cluster excess ($n_{\text{ON}} - n_{\text{OFF}}$), fitted excess (equation 4.2) and 99% C.L. upper limit on the cluster excess (equation 4.4) as function of cluster size for $\Delta t = 60$ s. The standard deviation of the n_{OFF} distribution is shown as error bars.

depends on the assumed particle physics model. The upper limits on $\dot{\rho}_{\text{PBH}}$ derived in section 5.1 were obtained with the standard model of particle physics (section 3). Because of equation 5.1, the PBHs evaporating at the present moment were initially in a very narrow range of masses if they formed at about the same time. At the cost of additional hypotheses on the PBH mass distribution, it is possible to use our measurements to constrain the initial contribution of these PBHs to the dark matter (DM). A recent review of PBH as dark matter is given in [33]. Popular models for the initial mass distribution of PBHs are the log-normal and the power-law distributions [34]. The latter is the simplest model for the initial mass distribution of PBHs and describes their production in the early universe by scale-invariant Gaussian density perturbations. It is given by [11]:

$$\frac{d\mathcal{N}_{\text{PBH}}}{dM_i} = \frac{\rho_0}{M_*} \left(\frac{M_i}{M_*} \right)^{-\beta}, \quad (5.2)$$

where M_i is the initial mass of PBHs, $M_* \simeq (0.5 - 1) \times 10^{15} \text{g}$ is the initial mass of a PBH that formed in the early universe and is, at the present time, at the final stage of its evaporation and β is the index of the initial PBH mass function, which is constrained to be larger than 2 and has a value of 2.5 in the radiation-dominated era [34]. In equation 5.2, \mathcal{N}_{PBH} is the number density of PBHs.

The normalization factor ρ_0 is given by

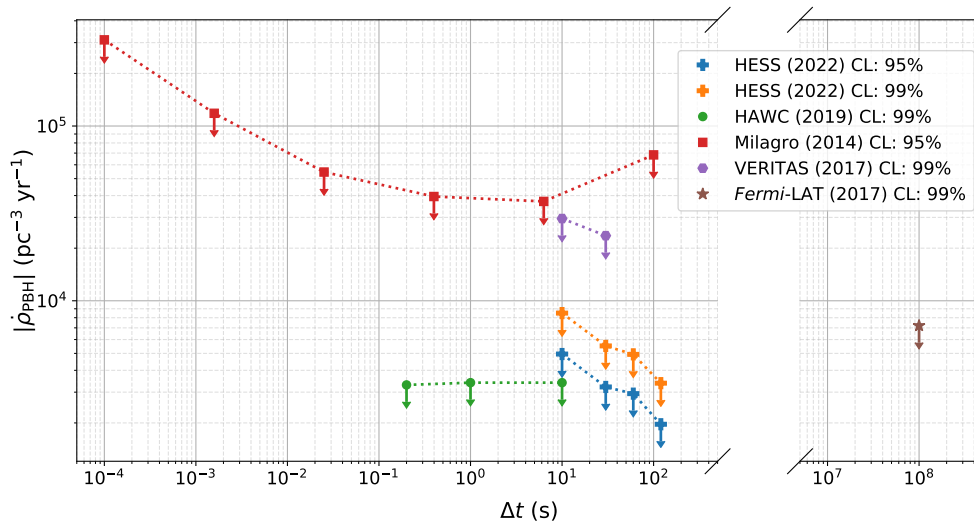


Figure 4: Upper limits on the PBH evaporation burst rate $\dot{\rho}_{\text{PBH}}$ for burst time scales of 10, 30, 60 and 120 seconds measured by H.E.S.S. Upper limits from HAWC [10], VERITAS [8], Milagro [32] and Fermi-LAT [9] are also shown.

$$\rho_0 = (\beta - 2) \frac{\Omega_{\text{PBH}} \rho_c}{M_*}, \quad (5.3)$$

where Ω_{PBH} is the fraction of the critical density ρ_c in PBHs with mass larger than M_* . Equation 12 from [11] gives the current local rate of vanishing PBHs as:

$$|\dot{\rho}_{\text{PBH}}| \simeq \frac{\alpha(M_*)}{M_*^3} \eta \rho_0, \quad (5.4)$$

where η , the clustering factor, is the ratio between the local and global dark matter densities.

Upper limits on the initial PBH mass fraction Ω_{PBH} as a function of the index β can be obtained from equations 5.3 and 5.4 taking, for $M_* = 10^{15}$ g, η to be its 95 % CL limit value $\eta > 1.6 \times 10^4$ [35] and $\alpha(M_*) > 10^{17}$ kg³ s⁻¹ [11]. Results are shown in Figure 5. In the scenario of PBH formation from density fluctuations, the initial mass fraction in PBHs with mass larger than M_* is constrained to be a subdominant fraction of the dark matter for most values of the β exponent.

Alternatively, fixing β gives a constraint on the present density of low-mass PBHs. Figure 6 shows the 95% confidence limits on the present density of PBHs derived from the limit on the present rate of evaporation bursts. β was varied between 2 and 3. For each value of β , an effective monochromatic PBH mass was calculated according to the prescription of [36]. The burst limit is compared to limits obtained from the Galactic and extra-galactic gamma-ray backgrounds taken from [37]. The H.E.S.S. limit is much less constraining than those derived from the gamma-ray background measurements. But the H.E.S.S. measurement is local, sensitive to PBHs located within 0.1 pc from the Sun, and is sensitive only to the initial value M_* of presently evaporating PBHs. In contrast, gamma-ray background limits on Ω_{PBH} are sensitive to PBHs in much larger volumes, but also to details of the low-mass tail of the initial and evolved mass distribution of PBHs.

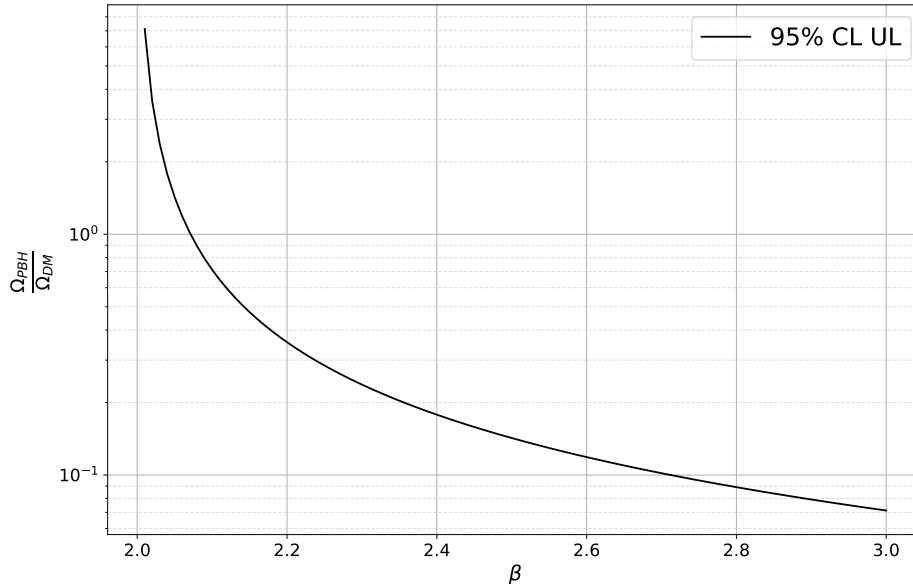


Figure 5: Upper limits on the initial PBH fraction of the dark matter density as a function of the PBH mass distribution index β .

6 Conclusions

The theory of Hawking radiation predicts that PBHs at their final stage of evaporation should produce bursts of high-energy particles. More than 4800 hours of H.E.S.S. observations have been used to search for short time-scale (10 s to 120 s) clusters of photons corresponding to the expected evaporation burst signal. The number of clusters found is fully compatible with statistical fluctuations with no significant signal. The most constraining 95% CL upper limit on the PBH burst rate was found to be $|\dot{\rho}_{\text{PBH}}| < 2000 \text{ pc}^{-3} \text{ yr}^{-1}$. This limit is comparable to those obtained by HAWC [10] and Fermi-LAT [9], taking into account the different signal prediction. Finally, the limit on the PBH evaporation rate has been translated into a constraint on the initial fraction of dark matter in PBHs of order $0.1 \Omega_{\text{DM}}$ for the hypothesis of a PBH initial mass power-law distribution. In the near future, the upcoming VHE gamma ray observatory CTA will be sensitive to a much larger fraction of the sky and should be able to lower the limit on the PBH burst rate obtained in the present paper by an order of magnitude if no bursts are detected [38].

Acknowledgments

The support of the Namibian authorities and of the University of Namibia in facilitating the construction and operation of H.E.S.S. is gratefully acknowledged, as is the support by the German Ministry for Education and Research (BMBF), the Max Planck Society, the German Research Foundation (DFG), the Helmholtz Association, the Alexander von Humboldt Foundation, the French Ministry of Higher Education, Research and Innovation, the Centre National de la Recherche Scientifique (CNRS/IN2P3 and CNRS/INSU), the Commissariat à l'énergie atomique et aux énergies alternatives (CEA), the

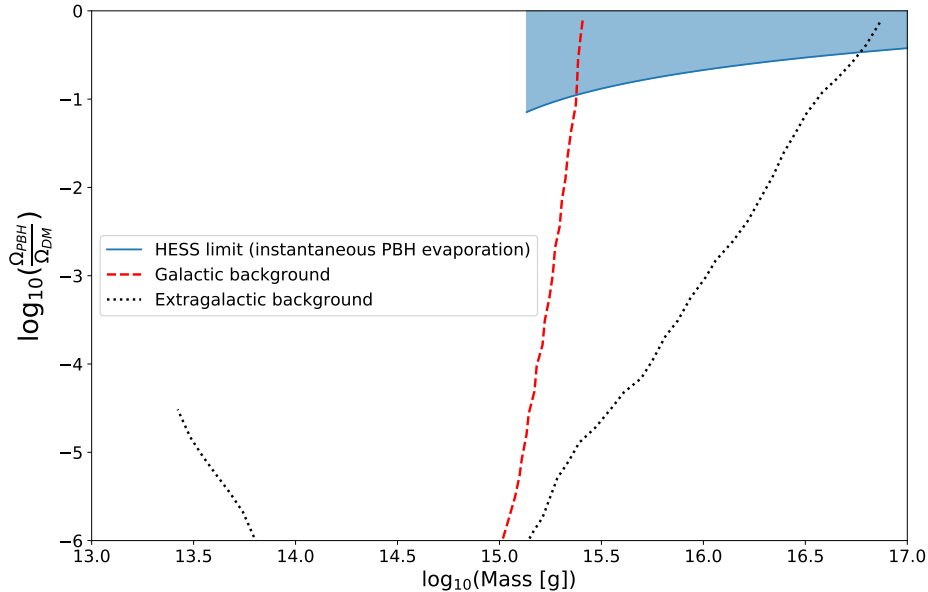


Figure 6: Upper limits on the present mass fraction of PBH as a function of the effective PBH mass. The initial mass distribution index β is varied between 2 and 3, giving the blue exclusion region. The limit is compared to monochromatic gamma-ray limits compiled in [37].

U.K. Science and Technology Facilities Council (STFC), the Irish Research Council (IRC) and the Science Foundation Ireland (SFI), the Knut and Alice Wallenberg Foundation, the Polish Ministry of Education and Science, agreement no. 2021/WK/06, the South African Department of Science and Technology and National Research Foundation, the University of Namibia, the National Commission on Research, Science & Technology of Namibia (NCRST), the Austrian Federal Ministry of Education, Science and Research and the Austrian Science Fund (FWF), the Australian Research Council (ARC), the Japan Society for the Promotion of Science, the University of Amsterdam and the Science Committee of Armenia grant 21AG-1C085. We appreciate the excellent work of the technical support staff in Berlin, Zeuthen, Heidelberg, Palaiseau, Paris, Saclay, Tübingen and in Namibia in the construction and operation of the equipment. This work benefited from services provided by the H.E.S.S. Virtual Organisation, supported by the national resource providers of the EGI Federation.

References

- [1] B. J. Carr and S. W. Hawking, *Black holes in the early Universe*, *MNRAS* **168** (1974) 399.
- [2] B. J. Carr, *Primordial Black Holes: Do They Exist and Are They Useful?*, *arXiv e-prints* (2005) astro [[astro-ph/0511743](#)].
- [3] A. M. Green and A. R. Liddle, *Constraints on the density perturbation spectrum from primordial black holes*, *Physical Review D* **56** (1997) 6166 [[astro-ph/9704251](#)].
- [4] K. Jedamzik, *Primordial black hole formation during the QCD epoch*, *Physical Review D* **55** (1997) 5871 [[arXiv:astro-ph/9605152](#)].

- [5] S. Bird, I. Cholis, J. B. Muñoz, Y. Ali-Haimoud, M. Kamionkowski, E. D. Kovetz et al., *Did LIGO Detect Dark Matter?*, *Physical Review Letters* **116** (2016) 201301 [[1603.00464](#)].
- [6] S. W. Hawking, *Black hole explosions?*, *Nature* **248** (1974) 30.
- [7] B. J. Carr, K. Kohri, Y. Sendouda and J. Yokoyama, *Constraints on primordial black holes from the Galactic gamma-ray background*, *Physical Review D* **94** (2016) 044029 [[1604.05349](#)].
- [8] S. Archambault and VERITAS Collaboration, *Search for Primordial Black Hole Evaporation with VERITAS*, in *35th International Cosmic Ray Conference (ICRC2017)*, vol. 301 of *International Cosmic Ray Conference*, p. 691, Jan., 2017, [1709.00307](#).
- [9] M. Ackermann, W. B. Atwood, L. Baldini, J. Ballet, G. Barbiellini, D. Bastieri et al., *Search for Gamma-Ray Emission from Local Primordial Black Holes with the Fermi Large Area Telescope*, *ApJ*. **857** (2018) 49.
- [10] A. Albert, R. Alfaro, C. Alvarez, J. C. Arteaga-Velázquez, K. P. Arunbabu, D. Avila Rojas et al., *Constraining the local burst rate density of primordial black holes with HAWC*, *JCAP* **2020** (2020) 026 [[1911.04356](#)].
- [11] F. Halzen, E. Zas, J. H. MacGibbon and T. C. Weekes, *Gamma rays and energetic particles from primordial black holes*, *Nature* **353** (1991) 807.
- [12] K. Bernlöhr, O. Carrol, R. Cornils, S. Elfahem, P. Espigat, S. Gillessen et al., *The optical system of the H.E.S.S. imaging atmospheric Cherenkov telescopes. Part I: layout and components of the system*, *Astroparticle Physics* **20** (2003) 111 [[arXiv:astro-ph/0308246](#)].
- [13] A. Daum, G. Hermann, M. Heß, W. Hofmann, H. Lampeitl, G. Pühlhofer et al., *First results on the performance of the HEGRA IACT array*, *Astroparticle Physics* **8** (1997) 1.
- [14] M. de Naurois and L. Rolland, *A high performance likelihood reconstruction of γ -rays for imaging atmospheric Cherenkov telescopes*, *Astroparticle Physics* **32** (2009) 231 [[0907.2610](#)].
- [15] R. D. Parsons and J. A. Hinton, *A Monte Carlo template based analysis for air-Cherenkov arrays*, *Astroparticle Physics* **56** (2014) 26 [[1403.2993](#)].
- [16] S. Ohm, C. van Eldik and K. Egberts, *γ /hadron separation in very-high-energy γ -ray astronomy using a multivariate analysis method*, *Astroparticle Physics* **31** (2009) 383 [[0904.1136](#)].
- [17] R. Hagedorn, *Hadronic matter near the boiling point*, *Nuovo Cimento A Serie* **56** (1968) 1027.
- [18] M. Schroedter, F. Krennrich, S. Lebohec, A. Falcone, S. J. Fegan, D. Horan et al., *Search for primordial black holes with SGARFACE*, *Astroparticle Physics* **31** (2009) 102 [[0812.0546](#)].
- [19] A. Barrau and C. Rovelli, *Planck star phenomenology*, *Physics Letters B* **739** (2014) 405 [[1404.5821](#)].
- [20] J. H. MacGibbon and B. R. Webber, *Quark- and gluon-jet emission from primordial black holes: The instantaneous spectra*, *Physical Review D* **41** (1990) 3052.
- [21] T. N. Ukwatta, D. R. Stump, J. T. Linnemann, J. H. MacGibbon, S. S. Marinelli, T. Yapici et al., *Primordial Black Holes: Observational characteristics of the final evaporation*, *Astroparticle Physics* **80** (2016) 90 [[1510.04372](#)].
- [22] A. F. Heckler, *Formation of a Hawking-radiation photosphere around microscopic black holes*, *Physical Review D* **55** (1997) 480 [[arXiv:astro-ph/9601029](#)].
- [23] R. Daghigh and J. Kapusta, *High temperature matter and gamma ray spectra from microscopic black holes*, *Physical Review D* **65** (2002) 064028 [[arXiv:gr-qc/0109090](#)].
- [24] J. H. MacGibbon, B. J. Carr and D. N. Page, *Do evaporating black holes form photospheres?*, *Physical Review D* **78** (2008) 064043 [[0709.2380](#)].

- [25] E. T. Linton, R. W. Atkins, H. M. Badran, G. Blaylock, P. J. Boyle, J. H. Buckley et al., *A new search for primordial black hole evaporations using the Whipple gamma-ray telescope*, *JCAP* **2006** (2006) 013.
- [26] E. Bugaev, P. Klimai and V. Petkov, *Photon spectra from final stages of a primordial black hole evaporation in different theoretical models*, in *International Cosmic Ray Conference*, vol. 3 of *International Cosmic Ray Conference*, pp. 1123–1126, Jan., 2008, [0706.3778](#).
- [27] A. Arbey and J. Auffinger, *BlackHawk: a public code for calculating the Hawking evaporation spectra of any black hole distribution*, *European Physical Journal C* **79** (2019) 693 [[1905.04268](#)].
- [28] M. Ankerst, M. M. Breunig, H. Kriegel and J. Sander, *OPTICS: ordering points to identify the clustering structure*, in *SIGMOD 1999, Proceedings ACM SIGMOD International Conference on Management of Data, June 1-3, 1999, Philadelphia, Pennsylvania, USA*, A. Delis, C. Faloutsos and S. Ghandeharizadeh, eds., pp. 49–60, ACM Press, 1999, [DOI](#).
- [29] F. Pedregosa, G. Varoquaux, A. Gramfort, V. Michel, B. Thirion, O. Grisel et al., *Scikit-learn: Machine learning in python*, *CoRR* **abs/1201.0490** (2012) [[1201.0490](#)].
- [30] M. Ester, H. Kriegel, J. Sander and X. Xu, *A density-based algorithm for discovering clusters in large spatial databases with noise*, in *Proceedings of the Second International Conference on Knowledge Discovery and Data Mining (KDD-96), Portland, Oregon, USA*, E. Simoudis, J. Han and U. M. Fayyad, eds., pp. 226–231, AAAI Press, 1996, <http://www.aaai.org/Library/KDD/1996/kdd96-037.php>.
- [31] G. J. Feldman and R. D. Cousins, *Unified approach to the classical statistical analysis of small signals*, *Physical Review D* **57** (1998) 3873 [[physics/9711021](#)].
- [32] A. A. Abdo, A. U. Abeysekara, R. Alfaro, B. T. Allen, C. Alvarez, J. D. Álvarez et al., *Milagro Limits and HAWC Sensitivity for the Rate-Density of Evaporating Primordial Black Holes*, *Astroparticle Physics* **64** (2015) 4.
- [33] B. Carr and F. Kühnel, *Primordial Black Holes as Dark Matter: Recent Developments*, *Annual Review of Nuclear and Particle Science* **70** (2020) 355 [[2006.02838](#)].
- [34] N. Bellomo, J. L. Bernal, A. Raccanelli and L. Verde, *Primordial black holes as dark matter: converting constraints from monochromatic to extended mass distributions*, *JCAP* **2018** (2018) 004 [[1709.07467](#)].
- [35] J. Bovy and S. Tremaine, *On the Local Dark Matter Density*, *The Astrophysical Journal* **756** (2012) 89.
- [36] B. Carr, M. Raidal, T. Tenkanen, V. Vaskonen and H. Veermäe, *Primordial black hole constraints for extended mass functions*, *Physical Review D* **96** (2017) 023514 [[1705.05567](#)].
- [37] B. Carr, K. Kohri, Y. Sendouda and J. Yokoyama, *Constraints on primordial black holes*, *Reports on Progress in Physics* **84** (2021) 116902 [[2002.12778](#)].
- [38] M. Doro, M. A. Sánchez-Conde and M. Hütten, *Fundamental Physics Searches with IACTs*, *arXiv e-prints* (2021) arXiv:2111.01198 [[2111.01198](#)].